

The Possible Therapeutic Role of Mesenchymal Stem Cells of Bone Marrow in Treatment of Diabetic Nephropathy in Albino Rats

Hind H. Ahmed, Saleh S. Edris, Naglaa A. Sarg, Essam M. Mhlab, Hend R. Mousa

Department of Anatomy and embryology, Faculty of Medicine Benha University, Egypt.

Corresponding to: Hind H. Ahmed, Department of Anatomy and embryology, Faculty of Medicine Benha University, Egypt.

Email:
hind.hamdy@fmed.bu.edu.eg

Received: 25 January 2024

Accepted: 5 March 2024

Abstract

Background: Uncontrolled diabetes mellitus plays a significant role in the development of diabetic nephropathy. **Aim:** This study was performed to assess the pathological effect of diabetes on the kidney, the possible improvement of diabetic nephropathy by Insulin, and the therapeutic effect of mesenchymal stem cells. **Methods:** 50 healthy albino adult male rats were subdivided into two main groups, Group 1: control group (8 rats). Group 2: 42 rats were given a single intraperitoneal injection of streptozotocin (80 mg/kg). After 6 weeks, confirming diabetic nephropathy, rats were dispersed into 3 groups as follows; Group (2a): diabetic nephropathic untreated rats, Group (2b) was given insulin glargine 6 IU/24 hours, for 6 weeks and Group (2c) was received MSCs in intravenous injection (10^6 cells) per rat once. After sacrificing rats at the end of the experiment, blood sampling was done for laboratory analysis of serum urea, and creatinine. Kidney samples were prepared for light and electron microscopic examination. **Results:** Diabetic rats showed altered biochemical and histological changes which are dilated filtration space, focal lytic (degenerated) areas, and congested blood capillaries were observed in the diabetic group. Disfigurement of the renal tubules, with vacuolated cytoplasm in the insulin group while, normal appearance with mild increase in the Bowman's space in the MSCs group, with significant ameliorative effects on renal function. **Conclusion:** Treatment with insulin and MSCs showed improved histological and biochemical parameters in the kidneys of diabetic rats.

Keywords: Diabetic nephropathy, Insulin, Mesenchymal stem cells.

Introduction

Diabetes mellitus is characterized by hyperglycemia. Advanced glycation end products (AGEs) buildup and insufficient

control of glucose are major factors in the development of diabetic nephropathy. Furthermore, diabetes is the most common

cause of kidney failure⁽¹⁾. While intensive insulin therapy and other interventions slow the development of diabetic complications, there is far less evidence that these interventions reverse diabetic complications⁽²⁾.

Mesenchymal stem cells (MSCs) have several advantages for therapeutic use, such as ease of harvesting, multilineage differentiation potential, and the lack of ethical issues that occur with the application of human embryonic stem cells (ESCs). In the past decades, the therapeutic value of MSCs has been extensively assessed in a broad range of disease models and clinical trials⁽³⁾.

Materials and methods

I-Materials:

This study is experimental research approved by the Research Ethics Committee of faculty of Medicine, Benha University (MD-2-11-220)

1. Animals

This study was carried out on 50 adult albino rats, weighing between 200 and 250 mg, obtained from laboratory animal house unit of Kasr Al-Ainy Faculty of Medicine, Cairo University and housed in plastic cages at $20 \pm 2^\circ\text{C}$ and 14 h: 10 h light: dark, Rats were fed a standard diet and water, at the laboratory animal house unit of Kasr Al-Ainy, Faculty of Medicine, Cairo University. The experimental protocol was approved by the Research Ethical Committee of the Faculty of Medicine, Benha University. After an accommodation period of 1 week,

the experiment was done from 5 January 2021 to 30 March 2021.

2. Chemicals

Streptozotocin: As a drug named Zanosar, it was obtained from Sigma Chemical Company (Sigma-Aldrich, St. Louis, MO) in the form of 1 gm white to yellow powder vial.

Insulin glargine: It is extended-action biosynthetic human insulin as a drug named Lantus, in the form of 10 ml vial containing 100 units/ ml.

3. Bone Marrow Mesenchymal Stem cells (BM-MSCs):

The BM-derived MSCs (which were processed and cultured for 14 days) were used in a single dose (1×10^6 cells/ ml) suspended in 1ml phosphate buffer saline (PBS) were injected intravenously in rat tail vein.

II- Methods:

1. Experimental design:

The fifty adult albino male rats were divided into two main groups:

Group 1 (control group): It consists of 8 healthy albino rats that weren't received any drugs.

Group 2 (Diabetic group): It consists of 42 Albino rats in which diabetes was induced by a single intra peritoneal injection of streptozotocin (STZ, 80 mg/kg; dissolved in citrate buffer (pH 4.5)⁽⁴⁾.

Three days after injections, diabetes was confirmed by the development of

hyperglycemia (blood glucose >300 mg/dl) in three successive days ⁽⁴⁾. Blood glucose was measured using a glucometer and its corresponding blood tests strips (Accu-Check; Roche Diagnostics, Germany) ⁽⁵⁾. Diabetic nephropathy (DN) was confirmed after 6 weeks of diabetic conformation by measuring serum urea and creatinine in blood ⁽⁶⁾.

The diabetic rats were randomly dispersed to 3 groups as follows: -

Group (2a): 14 diabetic untreated rats.

Group (2b): 14 diabetic rats which were treated with insulin glargine in dose 6 IU/24 hours for 6 weeks ⁽⁷⁾. The doses of insulin to be given were determined according to blood glucose concentrations. A pre-dose blood sample was obtained by tail bleeding to measure blood glucose to achieve strict glucose control ⁽⁴⁾.

Group (2c): 14 diabetic rats which received MSCs (which was processed and cultured for 14 days), in a single dose of (106cells) per rat by intravenous injection in rat tail vein ⁽⁶⁾.

At the end of the experiment, blood sampling through the retro-orbital vein was done for laboratory analysis of serum creatinine, and urea. Then, the rats were anesthetized via intraperitoneal injection of sodium pentobarbital (Nembutal, 30 mg/kg b.w.) for sacrificing. The anesthetized animals were killed by cervical dislocation. The abdomen was opened via ventral incision and the kidneys were removed, the left one was fixed in 2.5% glutaraldehyde,

and the right one was fixed in 10 % formalin solution for 48 hrs.

2. Histopathological study:

Kidneys samples have been prepared for a light microscopic study by fixation in 10 % formalin and were handled to make paraffin sections at 5 µm thickness. The sections were stained with:

- Hematoxylin and Eosin stain.
- Masson's Trichome.

Slide visualization and image photographing were performed in the Anatomy Department, Faculty of Medicine, Benha University, Egypt. For such purpose, Nikon Eclipse 80i upright microscope (Nikon Corporation, Japan) with a fitted digital camera, Toup CamTM Xcam full HD camera (ToupTek Europe, Ultramacro Ltd., UK) was used.

- Transmission electron microscopic (TEM) examination:

Ultrastructure examination of kidneys samples fixed in 2.5% glutaraldehyde was done according to ⁽⁸⁾; the ultrathin slices were studied in the faculty of medicine, at Tanta University, Egypt, using a TEM JEOL JEM-100 S.

3. Biochemical study ⁽⁶⁾:

Six weeks after Insulin treatment and MSCs injection, blood sampling through the retro-orbital vein. Serum urea and creatinine levels were measured using the conventional colorimetric method using QuantiChrom TM assay kit based on the improved Jung and Jaffe methods, respectively (DIUR- 500 and DICT-500).

These samples collected before sacrifice of rats.

4. **Morphometric study** ⁽⁹⁾:

Percentage of collagenous fibers area in sections stained with Masson's trichrome, using Leica Qwin 500 image analyzer computer system (Leica Microsystems Ltd, Cambridge, UK).

Statistical analysis:

The results were analyzed using SPSS version 19 (SPSS Inc., Chicago, Illinois, USA) and formulated as the mean \pm SD. ANOVA was employed to ascertain the statistical significance, followed by Tukey's multiple comparison tests. $p \leq 0.05$ was deemed significant ⁽¹⁰⁾.

Results

❖ **Histological results**

➤ **Hematoxylin and Eosin results:**

Control group 1:

The renal cortex showed a normal glomerular structure surrounded by Bowman's capsule. The proximal convoluted tubules had a preserved brush border, while the distal convoluted tubules had wider lumens and no brush borders (**Fig.1 a**)

Diabetic group(2a):

The renal cortex showed inflammatory cells infiltration, focal lytic areas and congested blood capillaries were observed. There was a dilatation of the filtration space. The nuclei of proximal and distal tubules appeared

pyknotic with vacuolated cytoplasm. Distorted proximal and dilated distal tubules were also observed (**Figs.1b**).

Diabetic group treated with insulin (group 2b):

The renal cortex exhibited mild increase in the Bowman's space of the glomerular structure. There was disfigurement of the renal tubules, with vacuolated cytoplasm (**Fig.1c**).

Diabetic group treated with mesenchymal stem cells (group 2c):

The renal cortex appeared to have normal proximal convoluted tubules with preserved brush borders and distal convoluted tubules. Additionally, the glomerular structure retained its normal appearance with mild increase in the Bowman's space (**Fig.1d**).

➤ **Masson's trichrome results:**

The renal cortex of the control and mesenchymal stem cell group exhibited thin blue collagen fibers surrounding tubules and renal glomeruli (**Figs.2 a& c**)

The diabetic and insulin group showed excess, blue-stained collagen fibers surrounding tubules and renal glomeruli in the renal cortex (**Figs.2 b& d**)

➤ **Transmission electron microscopic result:**

Control group 1:

The renal glomerulus showed Podocyte with euchromatic nucleus, resting on regular glomerular basement membrane (GBM) of

glomerular capillary with normal mitochondria (**Fig.3a**).

Proximal convoluted tubule (PCT) with characteristic apical long microvilli, central rounded euchromatic nucleus, nucleolus, elongated mitochondria, regular basal lamina, lysosomes, and intact junctional complex between the cells (**Fig.4a**).

Distal convoluted tubule (DCT) with short microvilli lining the lumen, normal nucleus, normal basal infoldings, mitochondria and Golgi apparatus were detected (**Fig.5a**).

Diabetic group(2a):

The renal glomerulus showed Podocyte with indented irregular dark nucleus, primary thick foot process and effacement of secondary foot processes. Increased thickness of glomerular basement membrane. Also, expansion of mesangial matrix was detected (**Fig.3b**).

PCT cell with focal loss of apical microvilli and loss of the basal infoldings. The rarified cytoplasm showed pyknotic nucleus, partial lysis of cristae of swollen mitochondria and cytoplasmic vacuolation (**Fig.4b**).

DCT showed widening in the intracellular spaces between the cells, disrupted basal infoldings. The rarified cytoplasm showed irregular small nucleus, degenerated mitochondria and cytoplasmic vacuolation (**Fig.5b**).

Diabetic group treated with insulin (group 2b):

The renal glomerulus showed Podocyte and its related blood capillary with irregular

endothelial cells and shrunken irregular pyknotic nucleus. Some areas of glomerular basement membrane (GBM) still have thickened areas and partial effacement of secondary foot process (**Fig.3c**).

PCT with long microvilli with central rounded nucleus, mild lysis in cytoplasm, normal mitochondria and slightly dilated SER. Large vacuoles were observed in cytoplasm (**Fig.4c**).

DCT showed lytic area in cytoplasm, irregular nucleus, disruption in the basal enfolding and degenerated mitochondria. Cytoplasmic vacuolation and absence of microvilli were determined (**Fig.5c**).

Diabetic group treated with mesenchymal stem cells (group 2c):

The renal glomerulus showed Podocyte with nearly normal nucleus, primary thick foot process and numerous secondary foot processes resting on GBM of glomerular capillary was detected. Capillary showed mesangial cells (**Fig.3d**).

PCT with regular euchromatic nucleus with extended chromatin, nucleolus, continuous long microvilli, normal mitochondria, smooth endoplasmic reticulum, regular basal lamina, and apical lysosomes. Normal appearance of lipid droplet was detected (**Fig.4d**).

DCT showed cells with regular normal nucleus with nucleolus, mitochondria, regular basal lamina, and characteristic short microvilli lining lumen was seen (**Fig.5d**).

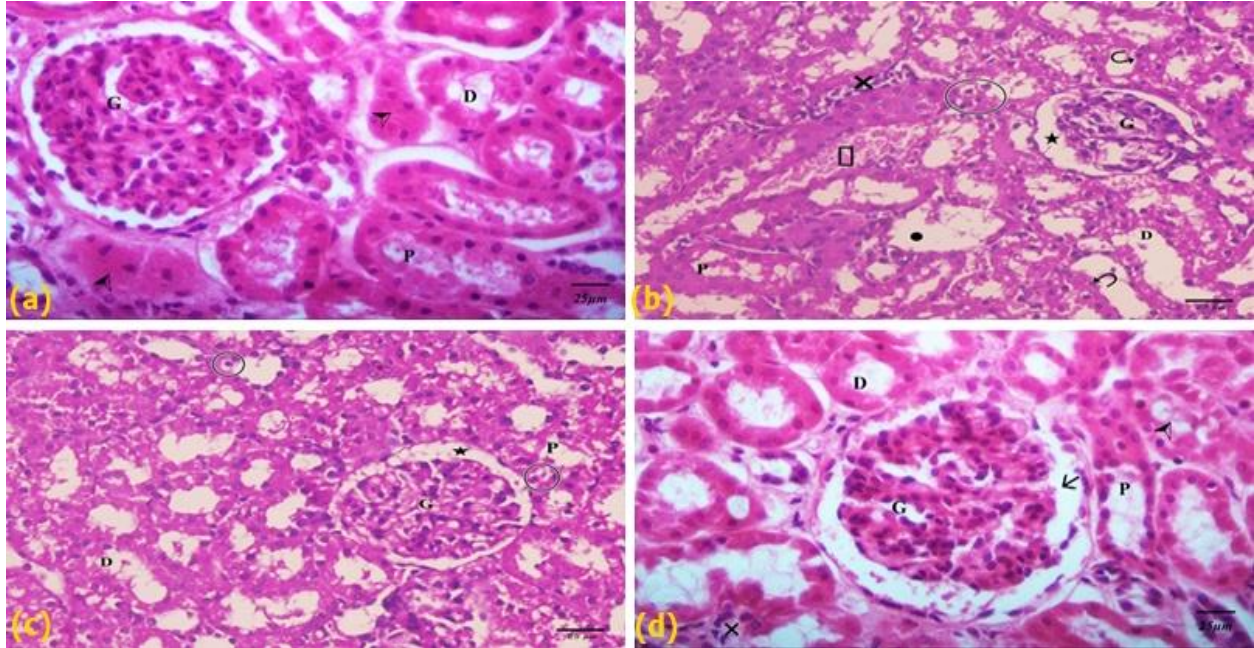


Fig. (1) (a): A photomicrograph of a section of the renal cortex of rat of control group 1 showing normal glomerular structure (G), proximal convoluted tubules (P) with intact brush border (arrowhead). The distal convoluted tubules (D) can be seen. **(H&E X400)**

Fig. (1) (b): A photomicrograph of the section of renal cortex of diabetic rat (group 2a) showing vacuolated cytoplasm in some tubular cells (circle), distorted proximal (P) and dilated distal (D) tubules. Some nuclei of the tubules appear pyknotic (curved arrow). Atrophied glomerulus (G) widened filtration space (star) can be seen. There are inflammatory cells infiltration (cross), Focal lytic area (dot) and congested blood capillaries (rectangle). **(H&E X400)**

Fig. (1) (c): A photomicrograph of a section of renal cortex of diabetic rat treated by insulin (group 2b) showing mild increase in Bowman's space (star) of glomerular structure (G). The proximal (P) and distal convoluted tubules (D) showed disfigurement with vacuolated cytoplasm (circle). **(H&E X400)**

Fig. (1) (d): A photomicrograph of a section of renal cortex of diabetic rat treated by mesenchymal stem cells (group 2c) showing mild infiltration with inflammatory cells (cross) in between convoluted tubules, nearly normal glomerular structure (G) with mild increase in Bowman's space (arrow). Proximal convoluted tubules (P) are intact with preserved brush border (arrowhead), distal convoluted tubules (D) can be observed in normal shape. **(H&E X400)**

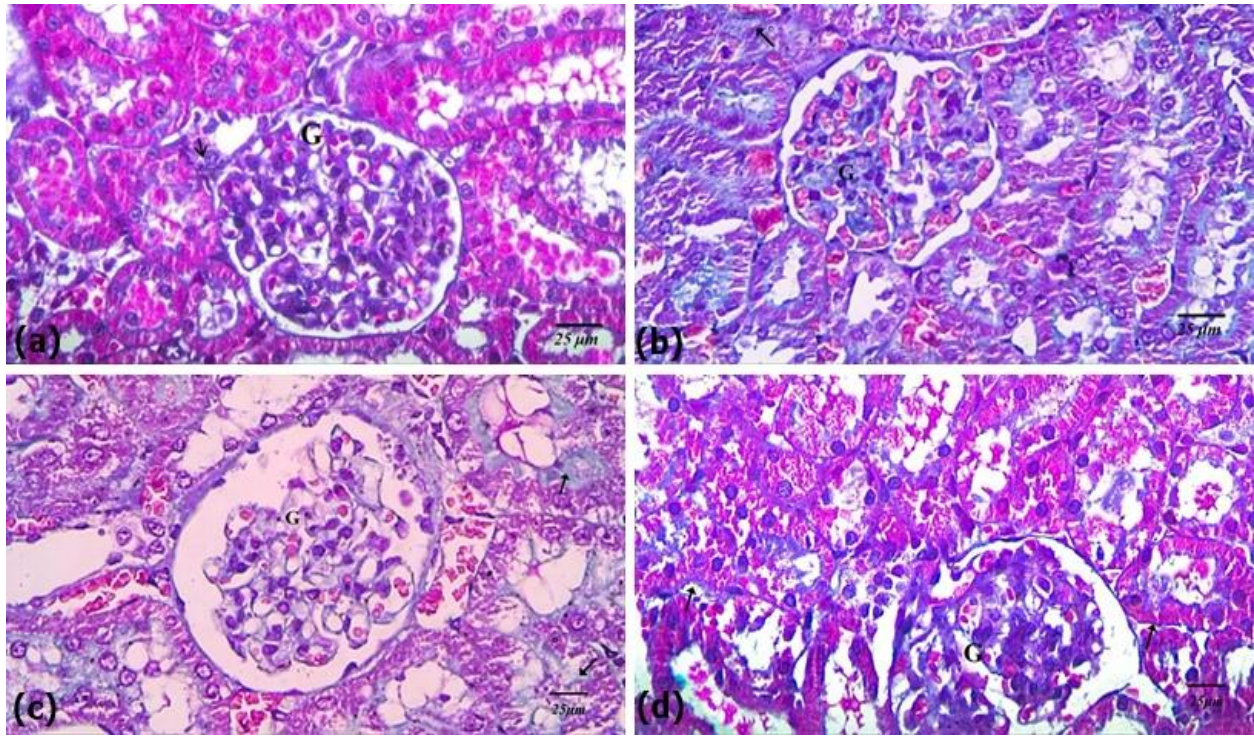


Fig. (2) (a): A photomicrograph of a section in the renal cortex of control group 1 showing thin blue collagen fibers around tubules (arrow) and renal glomeruli (G). (**Masson's Trichrome X400**)

Fig. (2) (b): A photomicrograph of the section of renal cortex of diabetic rat (group 2a) showing excess, blue-stained collagen fibers around the tubules (arrow) and renal glomeruli (G). (**Masson's Trichrome X400**)

Fig. (2) (c): A photomicrograph of a section of renal cortex of diabetic rat treated by insulin (group 2b) showing excess, blue-stained collagen fibers around tubules (arrow) and renal glomeruli (G). (**Masson's Trichrome X400**)

Fig. (2) (d): A photomicrograph of a section of renal cortex of diabetic rat treated by mesenchymal stem cells (group 2c) showing minimal, blue-stained collagen fibers around and within tubules (arrow) and renal glomeruli (G). (**Masson's Trichrome X400**)

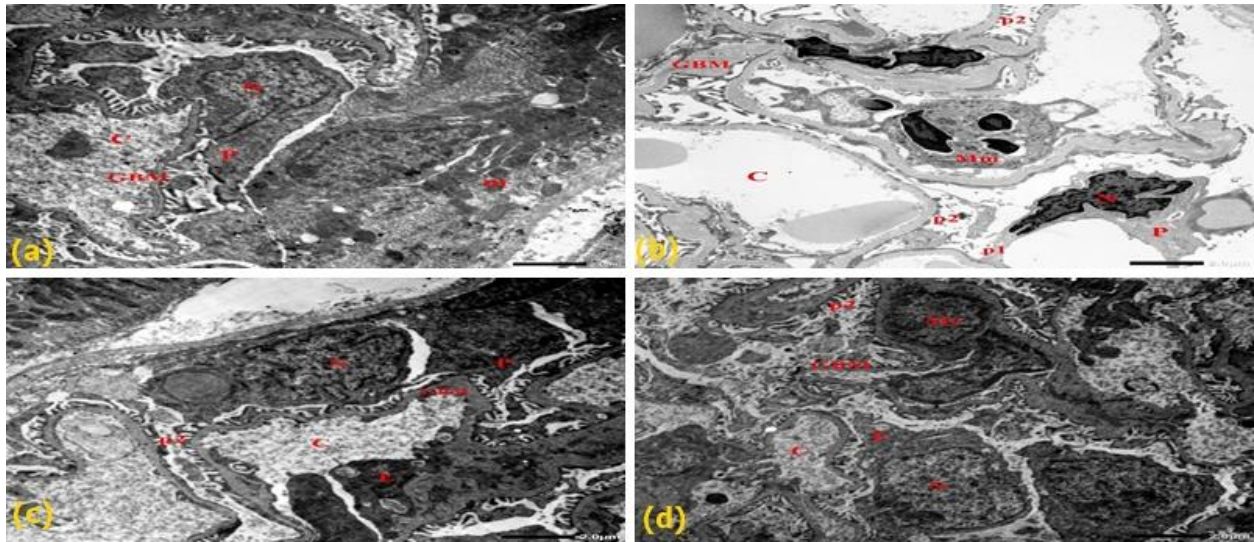


Fig. (3) (a): A photomicrograph of Transmission electron micrograph of the renal glomerulus of control group 1 showing Podocyte (P) with euchromatic nucleus (N), resting on regular glomerular basement membrane (GBM) (of glomerular capillary (C) with normal mitochondria (m). **(TEM X10000)**

Fig. (3) (b): A photomicrograph of Transmission electron micrograph of the renal glomerulus of diabetic rat (group 2a) showing Podocyte (P), its related blood capillary (C), primary thick foot process (p1) and detachment of secondary foot process (p2) with indented pyknotic nucleus (N). Increased thickness of glomerular basement membrane (GBM) and expansion of mesangial matrix (Mm) can be observed. **(TEM X10000)**

Fig. (3) (c): A photomicrograph of Transmission electron micrograph of the renal glomerulus of diabetic rat treated by insulin (group 2b) showing Podocyte (P) and its related blood capillary (c) with irregular endothelial cell (E) and shrunken irregular pyknotic nucleus (N). Some areas of glomerular basement membrane (GBM) still have thickened areas and partial effacement of secondary foot process (p2). **(TEM X10000)**

Fig. (3) (d): A photomicrograph of Transmission electron micrograph of the renal glomerulus of diabetic rat treated by mesenchymal stem cells (group 2c) showing Podocyte (p) and its related blood capillary (c) with secondary foot processes (p2) resting on normal basement membrane (GBM) with nearly normal nucleus (N). Capillary with mesangial cells (Mc) can be seen. **(TEM X10000)**

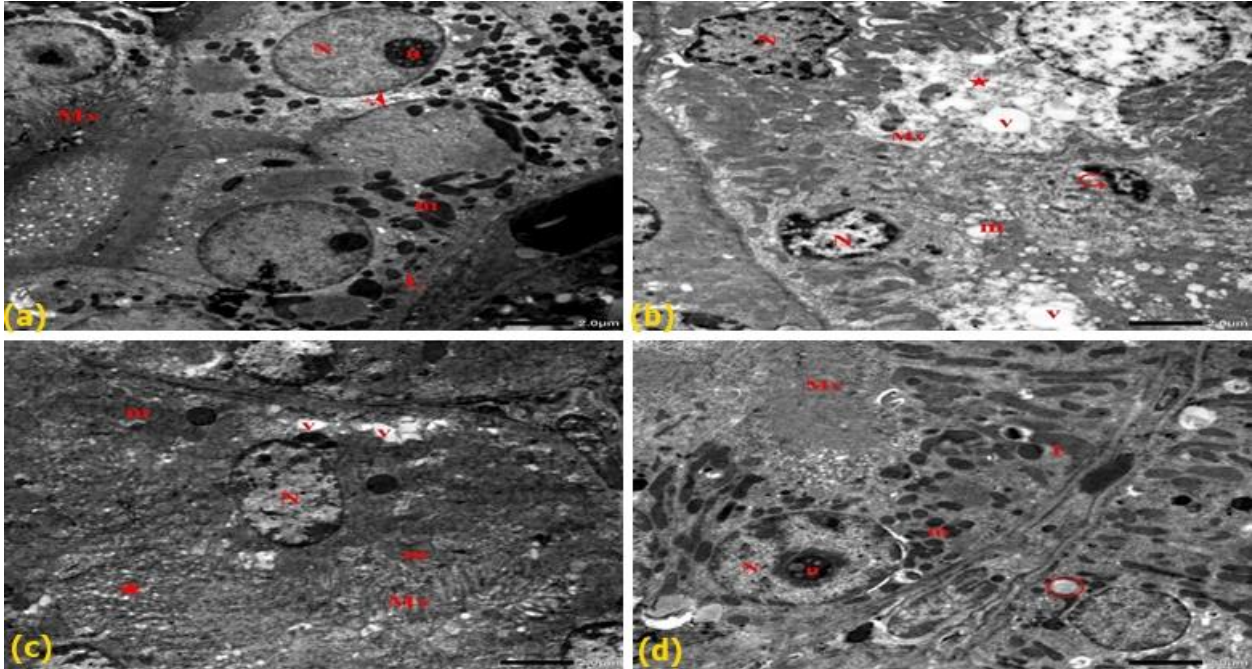


Fig. (4) (a): A photomicrograph of Transmission electron micrograph of the renal glomerulus of control group 1 showing cells of proximal convoluted tubules with characteristic apical long microvilli (Mv), central rounded euchromatic nucleus (N), with nucleolus (n). Elongated mitochondria (m), lysosomes (L) and intact junctional complex between the cells (arrowhead) can be seen. **(TEM X10000)**

Fig. (4) (b): A photomicrograph of Transmission electron micrograph of the renal glomerulus of diabetic rat (group 2a) showing PCT cells with focal loss of apical microvilli (Mv). The rarified cytoplasm (star) has pyknotic nucleus (curved arrow) and irregular one with extended chromatin (N), partial lysis of swollen mitochondria (m) and cytoplasmic vacuolation (V). **(TEM X10000)**

Fig. (4) (c): A photomicrograph of Transmission electron micrograph of the renal glomerulus of diabetic rat treated by insulin (group 2b) showing some cells of PCT having rarified cytoplasm (star), with some vacuoles (v), and characteristic apical continuous long microvilli (Mv). Normal central rounded nucleus (N), and normal mitochondria (m) can be noticed. **(TEM X10000)**

Fig. (4) (d): A photomicrograph of Transmission electron micrograph of the renal glomerulus of diabetic rat treated by mesenchymal stem cells (group 2c) showing most probably normal cell of PCT with regular euchromatic nucleus with extended chromatin (N), nucleolus (n). Continuous long microvilli (Mv), normal mitochondria (m) and lysosomes (L). Normal appearance of lipid droplets (circle) can be seen. **(TEM X10000)**

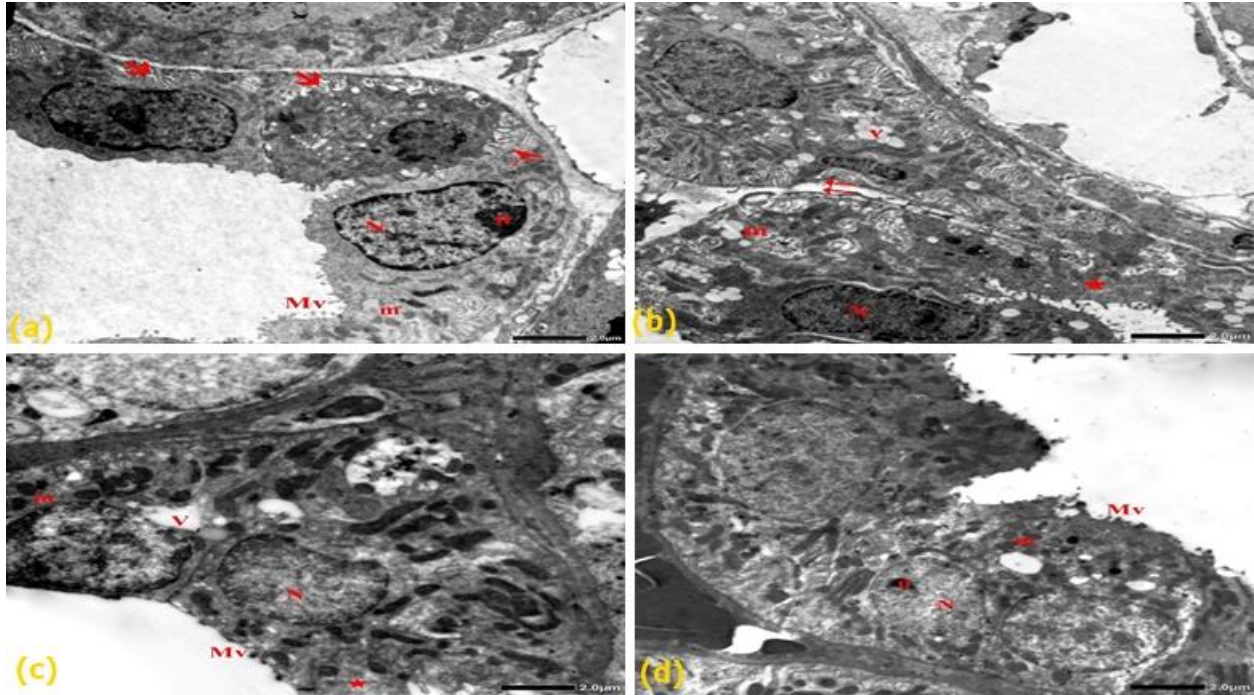


Fig. (5) (a): A photomicrograph of Transmission electron micrograph of the renal glomerulus of control group 1 showing distal convoluted tubules having lining cells with euchromatic nucleus (N), mitochondria (m). Normal basal membrane infoldings (arrow), intact junction between the cells (arrowhead) and short microvilli lining lumen (Mv). (TEM X10000)

Fig. (5) (b): A photomicrograph of Transmission electron micrograph of the renal glomerulus of diabetic rat (group 2a) showing DCT cell with widening in intercellular space between the cells (double arrow). The rarified cytoplasm (star) shows dark pyknotic nucleus (N), degenerated mitochondria (m) and vacuolations. (TEM X10000)

Fig. (5) (c): A photomicrograph of Transmission electron micrograph of the renal glomerulus of diabetic rat treated by insulin (group 2b) showing DCT cells with lytic area in cytoplasm (star), shrunken nucleus (N), and degenerated mitochondria (m), Cytoplasmic vacuolation (V) and partial absence of apical microvilli (Mv). (TEM X10000)

Fig. (5) (d): A photomicrograph of Transmission electron micrograph of the renal glomerulus of diabetic rat treated by mesenchymal stem cells (group 2c) showing nearly normal DCT cells with regular normal nucleus (N) with nucleolus (n), mitochondria (m), and characteristic short apical microvilli (Mv). (TEM X10000)

Biochemical results:

Mean values of serum urea level (Table 1)

Diabetic group (group2a) showed significant increase ($P < 0.05$) of serum urea level when compared with control group 1, diabetic rat treated by insulin (group 2b) and diabetic rat treated by mesenchymal stem cells (group 2c)

Diabetic rat treated by insulin (group 2b) showed increase ($P < 0.05$) of serum urea level when compared with control group 1 and significant decrease when compared with diabetic group (group2a)

Diabetic rat treated by mesenchymal stem cells (group 2c) showed significant decrease ($P < 0.05$) of serum urea level when compared with diabetic group (group2a).

Mean values of serum creatinine level (Table 2):

Diabetic group (group2a) showed significant increase ($P < 0.05$) of serum creatinine level when compared with control group 1, diabetic rat treated by insulin (group 2b) and diabetic rat treated by mesenchymal stem cells (group 2c)

Diabetic rat treated by insulin (group 2b) showed increase ($P < 0.05$) of serum creatinine level when compared with control

group, diabetic rat treated by mesenchymal stem cells (group 2c), and significant decrease when compared with diabetic group (group2a)

Diabetic rat treated by mesenchymal stem cells (group 2c) showed significant decrease ($P < 0.05$) of serum creatinine level when compared with diabetic group (group2a) and rat treated by insulin (group 2b).

Mean area percentage of collagen fiber deposition by Masson's trichrome staining (Table 3):

Diabetic group (group2a) showed significant increase ($P < 0.05$) of collagen fiber deposition when compared with control group 1, diabetic rat treated by insulin (group 2b) and diabetic rat treated by mesenchymal stem cells (group 2c)

Diabetic rat treated by insulin (group 2b) showed increase ($P < 0.05$) of collagen fiber deposition when compared with control group, diabetic rat treated by mesenchymal stem cells (group 2c), and significant decrease when compared with diabetic group (group2a)

Diabetic rat treated by mesenchymal stem cells (group 2c) showed significant decrease ($P < 0.05$) of collagen fiber deposition when compared with diabetic group (group2a) and rat treated by insulin (group 2b).

Table (1) shows mean values of serum urea level:

Mean % ± SD	Group 1 (control group)	Group 2a (diabetic group)	Group 2b (insulin group)	Group 2c (mesenchymal stem cell group)
Serum urea level (mg/dl)	14±3.5	26.5 ± 1.6	21.7 ± 3.3	17.3 ± 2
Significance ≤ 0.05	With groups 2a & 2b	With group 1, 2b & 2c	With groups 1, 2a	With group 2a

Table (2) show mean values of serum creatinine level:

Mean % ± SD	Group 1 (control group)	Group 2a (diabetic group)	Group 2b (insulin group)	Group 2c (mesenchymal stem cell group)
Serum creatinine level (mg/dl)	0.2±0.01	0.88±0.02	0.65 ± 0.04	0.29±0.09
Significance ≤ 0.05	With groups 2a & 2b	With groups 1, 2c & 2b	With Groups 1, 2a & 2c	With groups 2a& 2b

Table (3) show mean area percentage of collagen fiber deposition:

Mean % ± SD	Group 1 (control group)	Group 2a (diabetic group)	Group 2b (insulin group)	Group 2c (mesenchymal stem cell group)
Mean area percentage of collagen fibers deposition	4.1 ± 0.24 %	27.09 ± 0.28 %	14.87 ± 0.8 %	5.06 ± 0.3 %
Significance ≤ 0.05	With groups &2b	With groups 1, 2b & 2c	With groups 1, 2a & 2c	With groups 2a & 2b

Discussion

In the Present study, Streptozotocin-induced diabetic group showed glomerular affection, dilated filtration space, inflammatory cells infiltration and focal lytic areas in the cytoplasm of cells lining the proximal and distal tubules. These findings were in agreement with that published by ⁽¹¹⁾ and ⁽¹²⁾. The uncontrolled hyperglycemia triggered apoptotic changes through increase blood glucose level produces free radicals and reactive oxygen species (ROS), which activate oxidative stress and apoptosis of tubular epithelial cells and podocytes of the lipid peroxidation (LPO) level in the kidney was measured as malondialdehyde (MDA), which is the final product of lipid peroxidation. In diabetic rats, the antioxidant enzyme activities were significantly downregulated associated with an increase in malondialdehyde (MDA) level over the base line values ⁽¹³⁾.

Electron examinations of the renal cortex in diabetic rats in the current study showed that podocytes had an indented irregular dark nucleus and autophagic vacuole with primary thick foot processes and detachment of secondary foot processes. This result was similar to ⁽¹⁴⁾. Podocyte elimination is explained by ⁽¹⁵⁾ who reported that elevated glucose levels influence nephrin expression. Nephrin is a key podocyte protein that plays a direct role in actin dynamics and podocyte survival pathways. Podocytes became more susceptible to mechanical force-induced separation and the foot process was eliminated as a result.

In this study, the glomerular basement membrane (GBM) was irregularly thickened and there was an expansion of mesangial matrix in diabetic group. These findings were consistent with ⁽¹⁶⁾ and ⁽¹⁷⁾. Thickening of the GBM in DM, resulting from overproduction of matrix components and diminished matrix metalloproteinases (MMPs) activity which is important in extracellular matrix renovation ⁽¹⁸⁾.

In the current study, there was a significant increase in the area percent of collagen deposition noticed in diabetic rats. These results were similar to ⁽¹⁹⁾. According to ⁽²⁰⁾, tubular damage may trigger renal fibrosis and chronicity via inducing the tubular lining cells to release various mediators, including Tumor necrosis factor- α (TNF- α) which then promotes the differentiation and proliferation of myofibroblasts. ⁽²¹⁾ shown that in STZ-induced diabetic kidney nephropathy, ROS could activate nuclear factor-Kappa beta (NF- $\kappa\beta$), which up-regulates Transforming growth factor- β (TGF- β 1) which is a fibrogenic growth factor participates in progressive renal tubular atrophy.

In the current study, the histological changes were consistent with the significant elevation of urea and creatinine in the diabetic group when compared with control group. These results are consistent with findings of ⁽²²⁾ and ⁽¹⁸⁾ who reported impaired the renal functions of the DM rats indicated by increase of serum levels of creatinine, urea. ⁽²³⁾ reported that three weeks of diabetic induction is sufficient to cause oxidative stress that causes lipid peroxidation and renal damage, this is

demonstrated with high level of urea and creatinine.

In hematoxylin and eosin-stained sections of the renal cortex, treatment with insulin for six weeks after the creation of diabetic nephropathy model revealed some histopathological changes were still present as a mild increase in Bowman's space and disfigurement with vacuolation in the epithelial lining of the proximal and distal convoluted tubules. These results were in line with those of ⁽²⁴⁾, who found that insulin therapy partially restored the morphology of certain glomeruli and some proximal and distal convoluted tubules. However, several histological changes continued, including vacuolation in the tubule lining. Insulin treatment slowed the progress of diabetic nephropathy, stopped thickening of the glomerular basement membrane, and reduced tubular epithelial apoptosis ⁽²⁵⁾.

In this study, the ultrastructure of renal cortex of insulin treated group showed that podocyte had shrunken irregular pyknotic nucleus with irregular endothelial cell. Some areas of glomerular basement membrane still have thickened areas and partial effacement of secondary foot process. These results were in consistent with ⁽²⁶⁾ and ⁽²⁷⁾. Insulin is crucial for the regulation of glucose transferring and cytoskeletal contractility in podocytes due to highly expression of insulin receptor ⁽²⁶⁾.

The area percentage of collagen in insulin treated group significantly decreased when compared with diabetic group but still significantly increased when compared with control group. These results were explained by ⁽²⁸⁾ and ⁽²⁶⁾ that stated that insulin

decreases Alpha smooth muscle actin (α -SMA) and collagen I expression levels and increase nephrin expression at the mRNA and protein levels in podocytes.

According to the current study, the mean serum urea and creatinine level of the insulin group significantly decrease ($P < 0.05$) when compared with diabetic group but still significantly increase ($P < 0.05$) when compared with control group. These findings were consistent with ⁽²⁴⁾ who reported that treatment of diabetic nephropathy model with insulin showed improved oxidative reaction by decrease MDA level.

In this study, Hematoxylin and Eosin-stained sections of the renal cortex of MSCs treated group showed partially restored shape of some proximal, distal convoluted tubules and some glomeruli. These findings were similar to ⁽²⁹⁾ and ⁽³⁰⁾.

These results were explained by ⁽³¹⁾ who suggested that when the body ischemia, hypoxia, and injury, MSCs have a "homing" trait that predominately distributes to the injury site. Many researchers believe that the homing ability of MSCs may be the key to their therapeutic effect.

In this study, ultrastructure the renal cortex of MSCs treated group, revealed podocyte had a nearly normal nucleus, a primary thick foot process, and numerous secondary foot processes resting on the GBM of the glomerular capillary. These results were in agreement with ⁽²⁹⁾, ⁽³²⁾ and ⁽³³⁾.

In the current study, the area percent of collagen fibers in MSCs treated group

showed significant decrease ($P < 0.05$) when compared with diabetic and insulin treated groups, these results were similar to (34) who suggested that the improvement effect of MSCs on renal fibrosis in DN rats might be associated with significant suppression of high glucose-induced production of pro inflammatory cytokines (IL-6, IL-1 β , TNF- α) and profibrotic factor (TGF- β).

Based on the current study, MSCs treated group showed significant decrease in serum urea and creatinine levels ($P < 0.05$) when compared with diabetic group.

These results are consistent with findings from (35) and (36). (37) suggested that MSCs could hinder activation of NF-kB signal cascade by ROS as well as upregulation of TGF- β 1 and hyperglycemia-mediated in DN.

Conclusions

From this study, we concluded that treatment with insulin showed minimal improvement in the changes in glomerular structure, PCT, and DCT, compared with untreated diabetic rats.

Considering the efficacy of stem cell therapy, the current results showed a significant ameliorative effect on all histopathological features and biochemical markers as well as on the kidneys of diabetic rats.

References

1. Mestry SN, Dhodi JB, Kumbhar SB, Juvekar AR. Attenuation of diabetic nephropathy in streptozotocin-induced diabetic rats by Punica granatum Linn. leaves extract. *J Tradit Complement Med.* 2017;7(3):273–80.

2. Poplawski MM, Mastaitis JW, Isoda F, Grosjean F, Zheng F, Mobbs CV. Reversal of diabetic nephropathy by a ketogenic diet. *PloS One.* 2011;6(4):e18604.
3. Liu Y, Tang SC. Recent progress in stem cell therapy for diabetic nephropathy. *Kidney Dis.* 2016;2(1):20–7.
4. Etoh T, Inoguchi T, Kakimoto M, Sonoda N, Kobayashi K, Kuroda J, et al. Increased expression of NAD (P) H oxidase subunits, NOX4 and p22phox, in the kidney of streptozotocin-induced diabetic rats and its reversibility by interventive insulin treatment. *Diabetologia.* 2003;46(10):1428–37.
5. Cha KH, Jensen GC, Balijepalli AS, Cohan BE, Meyerhoff ME. Evaluation of Commercial Glucometer Test Strips for Potential Measurement of Glucose in Tears. *Anal Chem.* 2014 Feb 4;86(3):1902–8.
6. Abdel Aziz MT, Wassef MAA, Ahmed HH, Rashed L, Mahfouz S, Aly MI, et al. The role of bone marrow derived-mesenchymal stem cells in attenuation of kidney function in rats with diabetic nephropathy. *Diabetol Metab Syndr.* 2014 Dec;6(1):1–10.
7. Luippold G, Bedenik J, Voigt A, Grempler R. Short-and longterm glycemic control of streptozotocin-induced diabetic rats using different insulin preparations. *PloS One.* 2016;11(6):e0156346.
8. Abdulqadir SZ, Aziz FM. Internalization and effects on cellular ultrastructure of nickel nanoparticles in rat kidneys. *Int J Nanomedicine.* 2019 May 29;14:3995–4005.
9. Elsherbiny NM, El-Sherbiny M, Said E. Amelioration of experimentally induced diabetic nephropathy and renal damage by nilotinib. *J Physiol Biochem.* 2015;71(4):635–48.
10. Li Y, Liu J, Liao G, Zhang J, Chen Y, Li L, et al. Early intervention with mesenchymal stem cells prevents nephropathy in diabetic rats by

- ameliorating the inflammatory microenvironment. *Int J Mol Med*. 2018;41(5):2629–39.
11. Xie R, Zhang H, Wang X zhou, Yang X zhong, Wu S nong, Wang H gang, et al. The protective effect of betulinic acid (BA) diabetic nephropathy on streptozotocin (STZ)-induced diabetic rats. *Food Funct*. 2017;8(1):299–306.
 12. Chen J, Yang Y, Lv Z, Shu A, Du Q, Wang W, et al. Study on the inhibitive effect of Catalpol on diabetic nephropathy. *Life Sci*. 2020 Sep 15;257:118120.
 13. Ahmed ME, Gabr AEZ, Shams AM, Sherif RN, Taha RI. Dapagliflozin Versus Insulin: Which Is Better in Treatment of Diabetic Nephropathy in Albino Rats, Immunohistochemical Study. *Egypt Acad J Biol Sci Histol Histochem*. 2022 Jun 1;14(1):95–111.
 14. Sekiou O, Boumendjel M, Taibi F, Tichati L, Boumendjel A, Messarah M. Nephroprotective effect of *Artemisia herba alba* aqueous extract in alloxan-induced diabetic rats. *J Tradit Complement Med*. 2021 Jan 1;11(1):53–61.
 15. Huang H, Jiang Y, Mao G, Yuan F, Zheng H, Ruan Y, et al. Protective effects of allicin on streptozotocin-induced diabetic nephropathy in rats. *J Sci Food Agric*. 2017;97(4):1359–66.
 16. Saccon F, Gatto M, Ghirardello A, Iaccarino L, Punzi L, Doria A. Role of galectin-3 in autoimmune and non-autoimmune nephropathies. *Autoimmun Rev*. 2017;16(1):34–47.
 17. Tang F, Hao Y, Zhang X, Qin J. Effect of echinacoside on kidney fibrosis by inhibition of TGF- β 1/Smads signaling pathway in the db/db mice model of diabetic nephropathy. *Drug Des Devel Ther*. 2017 Sep 21;11:2813–26.
 18. Anders HJ, Huber TB, Isermann B, Schiffer M. CKD in diabetes: diabetic kidney disease versus nondiabetic kidney disease. *Nat Rev Nephrol*. 2018 Jun;14(6):361–77.
 19. Chang Y peng, Sun B, Han Z, Han F, Hu S lan, Li X yu, et al. Saxagliptin Attenuates Albuminuria by Inhibiting Podocyte Epithelial- to-Mesenchymal Transition via SDF-1 α in Diabetic Nephropathy. *Front Pharmacol* [Internet]. 2017 [cited 2023 Nov 14];8. Available from: <https://www.frontiersin.org/articles/10.3389/fphar.2017.00780>
 20. Li XQ, Chang DY, Chen M, Zhao MH. Deficiency of C3a receptor attenuates the development of diabetic nephropathy. *BMJ Open Diabetes Res Care*. 2019 Nov 1;7(1):e000817.
 21. Qi M you, He Y hao, Cheng Y, Fang Q, Ma R yu, Zhou S jie, et al. Icarin ameliorates streptozocin-induced diabetic nephropathy through suppressing the TLR4/NF- κ B signal pathway. *Food Funct*. 2021 Feb 15;12(3):1241–51.
 22. Saleh SS, Sarhat ER. Effects of ethanolic *Moringa oleifera* extract on melatonin, liver and kidney function tests in alloxan-induced diabetic rats. *Indian J Forensic Med Toxicol*. 2019;13(4):1015–9.
 23. Barutta F, Bellini S, Gruden G. Mechanisms of podocyte injury and implications for diabetic nephropathy. *Clin Sci*. 2022 Apr 13;136(7):493–520.
 24. Suanarunsawat T, Anantasomboon G, Piewbang C. Anti-diabetic and anti-oxidative activity of fixed oil extracted from *Ocimum sanctum* L. leaves in diabetic rats. *Exp Ther Med*. 2016 Mar 1;11(3):832–40.
 25. Aguilar C, Rodríguez-Delfin L. [Effects of spironolactone administration on the podocytes loss and progression of experimental diabetic nephropathy]. *Rev Peru Med Exp Salud Publica*. 2012 Oct 1;29(4):490–7.
 26. Meng F, Cao Y, Khoso MH, Kang K, Ren G, Xiao W, et al. Therapeutic effect and mechanism of combined use of FGF21 and insulin on diabetic nephropathy. *Arch Biochem Biophys*. 2021 Nov 30;713:109063.

27. Lu J, Chen PP, Zhang JX, Li XQ, Wang GH, Yuan BY, et al. GPR43 deficiency protects against podocyte insulin resistance in diabetic nephropathy through the restoration of AMPK α activity. *Theranostics*. 2021 Mar 4;11(10):4728–42.
28. Dong D, Fan T ting, Ji Y shi, Yu J yu, Wu S, Zhang L. Spironolactone alleviates diabetic nephropathy through promoting autophagy in podocytes. *Int Urol Nephrol*. 2019 Apr 1;51(4):755–64.
29. Ebrahim N, Ahmed IA, Hussien NI, Dessouky AA, Farid AS, Elshazly AM, et al. Mesenchymal Stem Cell-Derived Exosomes Ameliorated Diabetic Nephropathy by Autophagy Induction through the mTOR Signaling Pathway. *Cells*. 2018 Dec;7(12):226.
30. Hamza AH, Al-Bishri WM, Damiati LA, Ahmed HH. Mesenchymal stem cells: a future experimental exploration for recession of diabetic nephropathy. *Ren Fail*. 2017 Jan 1;39(1):67–76.
31. Xiang E, Han B, Zhang Q, Rao W, Wang Z, Chang C, et al. Human umbilical cord-derived mesenchymal stem cells prevent the progression of early diabetic nephropathy through inhibiting inflammation and fibrosis. *Stem Cell Res Ther*. 2020 Aug 3;11(1):336.
32. Wang S, Li Y, Zhao J, Zhang J, Huang Y. Mesenchymal stem cells ameliorate podocyte injury and proteinuria in a type 1 diabetic nephropathy rat model. *Biol Blood Marrow Transplant*. 2013;19(4):538–46.
33. Ding DC, Chang YH, Shyu WC, Lin SZ. Human Umbilical Cord Mesenchymal Stem Cells: A New Era for Stem Cell Therapy. *Cell Transplant*. 2015 Mar 1;24(3):339–47.
34. Xiong G, Tang W, Zhang D, He D, Wei G, Atala A, et al. Impaired Regeneration Potential in Urinary Stem Cells Diagnosed from the Patients with Diabetic Nephropathy. *Theranostics*. 2019 May 31;9(14):4221–32.
35. El-Tantawy WH, Haleem ENAA. Therapeutic effects of stem cell on hyperglycemia, hyperlipidemia, and oxidative stress in alloxan-treated rats. *Mol Cell Biochem*. 2014 Jun 1;391(1):193–200.
36. Lee KB, Choi J, Cho SB, Chung JY, Moon ES, Kim NS, et al. Topical embryonic stem cells enhance wound healing in diabetic rats. *J Orthop Res*. 2011;29(10):1554–62.
37. Ibrahim AAS, Morsy MM, Abouhashem SE, Aly O, Sabbah NA, Raafat N. Role of mesenchymal stem cells and their culture medium in alleviating kidney injury in rats diabetic nephropathy. *Egypt J Med Hum Genet*. 2020;21(1):1–13.

To cite this article: Hind H. Ahmed, Saleh S. Edris, Naglaa A. Sarg, Essam M. Mhlab, Hend R. Mousa. The Possible Therapeutic Role of Mesenchymal Stem Cells of Bone Marrow in Treatment of Diabetic Nephropathy in Albino Rats. *BMFJ* 2024;41(1):113-129.